University Library

MINERVA ACCESS

A gateway to Melbourne's research publications

Minerva Access is the Institutional Repository of The University of Melbourne

Author/s:
Catani, KJ;Sanelli, JA;Dryza, V;Gilka, N;Taylor, PR;Bieske, EJ

Title:
Electronic spectrum of the propargyl cation (H2C3H+) tagged with Ne and N2

Date:
2015-11-14

Citation:
Catani, K. J., Sanelli, J. A., Dryza, V., Gilka, N., Taylor, P. R. & Bieske, E. J. (2015). Electronic spectrum of the propargyl cation (H2C3H+) tagged with Ne and N2. Journal of Chemical Physics, 143 (18), https://doi.org/10.1063/1.4935169.

Persistent Link:
https://hdl.handle.net/11343/58277

Electronic spectrum of the propargyl cation ($H_2C_3H^+$) tagged with Ne and N_2

Katherine J. Catani,[1] Julian A. Sanelli,[1] Viktoras Dryza,[1] Natalie Gilka,[2] Peter R. Taylor,[1, a)] and Evan J. Bieske[1, b)]

[1)] *School of Chemistry, The University of Melbourne, Victoria, Australia 3010*

[2)] *School of Mathematics and Statistics, The University of Melbourne, Victoria, Australia 3010*

(Dated: 1 January 2016)

The $\tilde{A}^1A_1 \leftarrow \tilde{X}^1A_1$ band system of the propargyl cation ($H_2C_3H^+$) is measured over the 230-270 nm range by photodissociation of mass-selected $H_2C_3H^+$-Ne and $H_2C_3H^+$-N_2 complexes in a tandem mass spectrometer. The band origin occurs at 37 618 cm^{-1} for $H_2C_3H^+$-Ne and 37 703 cm^{-1} for $H_2C_3H^+$-N_2. Ground and excited state *ab initio* calculations for $H_2C_3H^+$ using the MCSCF and CC response methods show that the ion has C_{2v} symmetry in the ground $\tilde{X}^1A_1$ and excited $\tilde{A}^1A_1$ states and that the strong vibronic progression, with a spacing of 630 cm^{-1} is due to the C–C stretch vibrational mode, ν_5.

[a)] Electronic mail: prtaylor@unimelb.edu.au

[b)] Electronic mail: evanjb@unimelb.edu.au

I. INTRODUCTION

Although small hydrocarbon cations play important roles in combustion, plasmas and interstellar space, many are yet to be fully characterized from a spectroscopic standpoint. This is the case for the $C_3H_3^+$ ion, which, as shown in Fig. 1, has two energetically viable isomers, the cyclopropenyl cation (c-$C_3H_3^+$) and the propargyl cation ($H_2C_3H^+$). The c-$C_3H_3^+$ cation (D_{3h} symmetry) is the lower energy form and is the smallest aromatic system, with two π-electrons delocalized over the carbon framework. The $H_2C_3H^+$ cation (C_{2v} symmetry) lies 105 kJ/mol higher in energy and is more reactive than its cyclic counterpart.[1,2] Both isomers are commonly observed fragments in mass spectroscopy and can be distinguished by a difference in reactivities.[2] Furthermore, c-$C_3H_3^+$ and $H_2C_3H^+$ are considered to be important intermediates in combustion chemistry, playing a role in soot formation.[3] The two ions are also postulated to be present in the interstellar medium (ISM) and in planetary atmospheres.[4] The extraterrestrial presence of $C_3H_3^+$ has been confirmed by mass spectrometric observations of ions in the tail of the comet Halley.[5] $H_2C_3H^+$ and c-$C_3H_3^+$ are also predicted to play roles in the synthesis of cumulenic and cyclic C_3H_2, which are suspected to exist in large abundance in dark and diffuse clouds of the ISM.[6,7]

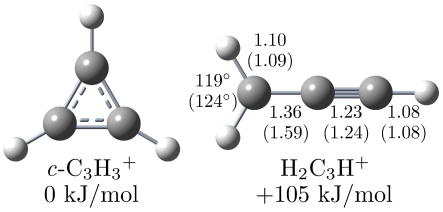


FIG. 1. The c-$C_3H_3^+$ and $H_2C_3H^+$ isomers. For $H_2C_3H^+$, calculated ground and excited state structural parameters are shown (bond lengths in Å, excited state parameters in parenthesis).

Due to its widespread relevance the propargyl cation has been the subject of theoretical investigations,[8–11] photoelectron studies,[12,13] IR spectroscopy,[14–17] and electronic spectroscopy.[16] Information on the ground state vibrational frequencies of $H_2C_3H^+$ has been derived from photoelectron spectra of H_2C_3H and through infrared photodissociation spectra of $H_2C_3H^+$ cations tagged with Ne, Ar, N_2, O_2 and CO_2.[9,14,15,17] These photodissociation spectra are congested and difficult to interpret in the CH stretch region due to the presence of both $H_2C_3H^+$ and c-$C_3H_3^+$ species and various isomers associated with the tag atom or molecule attached at different sites, and also by the occurrence of overtone and combinations

bands.

The $\tilde{A}^1A_1 \leftarrow \tilde{X}^1A_1$ electronic band system of $H_2C_3H^+$ in a Ne matrix was first measured by Wyss *et al.*[16] The band system, extending from 268 down to 240 nm, displayed a strong vibronic progression that was assigned to a CCH bending vibrational mode, implying a reduction of symmetry from the C_{2v} ground state to a C_s excited state. The observed bands were relatively broad, possibly concealing weaker transitions.

To further characterize the $H_2C_3H^+$ molecular cation we have measured the $\tilde{A}^1A_1 \leftarrow \tilde{X}^1A_1$ electronic spectra over the 235-270 nm range of the $H_2C_3H^+$-Ne and $H_2C_3H^+$-N_2 complexes by photodissociating them in a tandem mass spectrometer. The new photodissociation spectra exhibit more clearly resolved bands than the previous Ne matrix spectrum, providing a better view of the dominant progression, and allowing several new transitions to be observed. Complementary electronic structure calculations are conducted to provide structural parameters for $H_2C_3H^+$ in the ground and excited states and to assist in interpreting the measured spectra. An important aspect of the work is consideration of whether the extended vibronic progression in the $\tilde{A}^1A_1 \leftarrow \tilde{X}^1A_1$ electronic transition is indeed associated with a linear-bent transition accompanying a reduction in molecular symmetry from C_{2v} to C_s.

II. EXPERIMENTAL METHODS

The electronic spectrum of $H_2C_3H^+$ was recorded by resonance-enhanced photodissociation of the $H_2C_3H^+$-Ne and $H_2C_3H^+$-N_2 complexes in a tandem mass spectrometer, in each case by monitoring $H_2C_3H^+$ photofragments. The equipment has been described previously,[18–21] and here we provide only a brief outline. Vapour from a solution of propargyl bromide (C_3H_3Br) in toluene, cooled to 0°C, was seeded into a pulsed supersonic expansion of nitrogen or neon gas (backing pressure 4 bar) and bombarded with electrons to form the $H_2C_3H^+$ closed-shell cation. $H_2C_3H^+$-Ne or $H_2C_3H^+$-N_2 were formed through 3-body collisions in the free-jet expansion and mass-selected by a quadrupole mass filter. Charged complexes were then deflected 90° by an electrostatic quadrupole bender into an octopole ion guide and irradiated with light from a tuneable optical parametric oscillator (OPO, EKSPLA NT342B) with a bandwidth of $\approx 8\,cm^{-1}$. Resonant photoexcitation of $H_2C_3H^+$-Ne or $H_2C_3H^+$-N_2 generated $H_2C_3H^+$ photofragments that were mass-selected by a second quadrupole mass filter and detected by a microchannel plate. The $H_2C_3H^+$ ion signal was

monitored as the laser wavelength was scanned to record a photodissociation action spectrum, that was subsequently normalized with respect to laser power. Wavelength calibration was performed using a wavemeter (Ångstrom LSA UVL).

Note that we did not target the $C_3H_3^+$-Ar complex because of its near mass coincidence with the extremely abundant Ar_2^+ cation. Furthermore, we were unable to detect photodissociation of the untagged $C_3H_3^+$ cation.

There are several different possible photodissociation mechanisms. For example, electronically excited $H_2C_3H^+$-Ne or $H_2C_3H^+$-N_2 may undergo non-radiative decay to the ground state manifold, leading to rapid fragmentation of the vibrationally energized complex. It is also plausible that the complexes dissociate following fluorescence to excited vibrational levels in the ground state manifold lying above the dissociation threshold (D_e =241 and 1435 cm^{-1} for $H_2C_3H^+$-Ne and $H_2C_3H^+$-N_2, respectively[9]).

III. COMPUTATIONAL METHODS

The $H_2C_3H^+$ cation was examined computationally using several different approaches to determine ground and excited state structures and vibrational frequencies. Ground- and excited-state geometries and vibrational frequencies were calculated at the restricted active space self-consistent field (RASSCF)[22] level of theory using a cc-pVTZ basis set. State-averaging was not used: the ground- and excited-state wave functions were optimized in independent calculations as respectively the first and second roots of symmetry $^1A_1$. The active orbital space of 15 MOs (the three C 1s-derived MOs were held inactive) was partitioned as follows. The RAS1 space comprised four MOs of a_1 symmetry and one in b_2, the RAS2 space two in b_1 and two in b_2, and the RAS3 space four in a_1, and one each in b_1 and b_2. In essence, the RAS1 space described the σ-bonding orbitals, the RAS2 space the "in-plane" and out of plane π-bonding and antibonding orbitals, and the RAS3 space the remaining valence MOs. The RAS1 space was constrained to contain at least eight electrons, and the RAS3 space at most two. Compared to a full CASSCF calculation the RASSCF configuration space comprises some 7 000 configurations as opposed to well over 2 300 000: comparisons in a smaller atomic basis indicate that the difference in the calculated results is almost negligible. This RASSCF approach should give a balanced treatment of both states, but will necessarily suffer from the lack of dynamical correlation. In an attempt to

improve on these results we have performed CC3 linear response (CC3LR) calculations, in the cc-pVQZ basis, of the excitation energy, and have re-optimized the ground- and excited-state geometries using the CCSDT and EOM-CCSDT (CCSDT linear response, in effect) methods respectively, again in the cc-pVTZ basis. This should give a better estimate of the geometries — it is unfortunately not feasible to recompute the vibrational frequencies at this level.

The Dalton program[23] was used for the CASSCF and CC3/CC3LR energy calculations, and the CCSDT/EOM-CCSDT geometry optimizations were performed using CFOUR.[24] Vibrational modes were classified by their symmetries in the C_{2v} point group and numbered according to the Mulliken convention.[25]

The isomers of $H_2C_3H^+$-Ne and $H_2C_3H^+$-N_2 were characterized computationally by Botschwina and coworkers at the CCSD(T*)-F12a level giving relative energies and structures. However vibrational frequencies for the intermolecular modes were not reported. Therefore, the structures and vibrational frequencies of $H_2C_3H^+$-Ne and $H_2C_3H^+$-N_2 complexes were examined employing density functional theory (DFT) with the ωB97X-D functional[26] and aug-cc-pVTZ basis set. This level of theory, which incorporates empirical dispersion corrections, has been used for other charged non-covalently bound systems including quinoline$^+$-Ar and isoquinoline$^+$-Ar,[20] indene$^+$-Ar,[21] and indole$^+$-Ar.[27] These calculations were performed with the Gaussian 09 program suite.[28] Calculated vibrational frequencies of the complexes are provided in the supplemental material.[29]

IV. RESULTS AND DISCUSSION

A. Ground and excited state geometries, frequencies and excitation energies for $H_2C_3H^+$

The RASSCF/cc-pVTZ ground and excited state geometrical parameters for $H_2C_3H^+$ are shown in Fig. 1. Ground state structural parameters are very similar to those found through DFT/B3LYP/cc-pVTZ calculations by Ricks *et al.*[15] and the CCSD(T*)-F12a calculations by Botschwina *et al.*[8]

The predicted structural effects of exciting $H_2C_3H^+$ to the $\tilde{A}^1A_1$ state are summarized in Table I. The change in the first C–C bond length is particularly noteworthy. The excited

state wave function is dominated by excitation from the bonding π orbital to its antibonding counterpart and this substantially weakens the first C–C bond. Incidentally, the wave function contains significant contribution from the *double* excitation $\pi^2 \rightarrow \pi^{*2}$ as well as the corresponding single excitation, making it clear that this excited state is a poor candidate for single configuration-based methods such as LR-DFT. As expected, the weaker π bond results in a change in the angles around the methylene carbon, with the HCH angle opening by 5°. The calculated harmonic frequencies largely reflect expectations from the geometry changes from ground to excited state: modes expected to be largely unaffected by the weakening of the π bond have similar values between ground and excited state, whereas the C–C stretching frequency is predicted to decrease by over 400 cm^{-1}, and the C≡C stretch by 200 cm^{-1}, for example.

TABLE I. Differences between ground and excited state geometries at the RASSCF/cc-pVTZ and the CCSDT/EOM-CCSDT level. Bond lengths in Å and angles in degrees.

	ΔRASSCF	ΔCCSDT
r(C–C)	0.227	0.188
r(C≡C)	0.005	0.009
r(CH) (CH_2)	−0.006	−0.002
r(CH) (CH)	−0.002	−0.002
∠HCH	5.4	3.7

Improved geometry estimates from CCSDT calculations suggest that the increase in the C-C bond length as a result of excitation is somewhat overestimated by RASSCF: the latter suggests almost 0.23 Å increase whereas the CCSDT/EOM-CCSDT results suggest a smaller increase of 0.19 Å. This overestimation of the bond length change by RASSCF undoubtedly accounts for some of the discrepancies between the observed Franck-Condon profiles and those obtained by simulating the spectra as shown in the supplemental material.[29] Differences between the RASSCF and CCSDT/EOM-CCSDT results for the other geometry parameters are negligible at this level of accuracy.

At the CC3/CC3LR level, using the RASSCF-optimized geometries, the adiabatic T_e excitation energy is predicted to be 38 800 cm^{-1}, and using the RASSCF estimates for the zero-point vibrational contribution yields a T_0 value of 38 100 cm^{-1}. The vertical excitation

144 energy at the ground-state RASSCF geometry is predicted to be 41 100 cm^{-1}. We note that
145 these predictions are for the isolated $H_2C_3H^+$molecule, but the effect of the tethered species
146 on the excitation energy is expected to be minor and thus these results should be directly
147 relevant to the analysis of experiment here. Agreement appears to be within 1000 cm^{-1},
148 which is as good or better than would be expected for these methods.

TABLE II. Calculated harmonic vibrational frequencies for $H_2C_3H^+$ compared to experimental frequencies derived from spectra of $H_2C_3H^+$-Ar, $H_2C_3H^+$-Ne and $H_2C_3H^+$-N_2.

		$\tilde{X}^1A_1$		$\tilde{A}^1A_1$		
Mode	Description	Calc.[a]	Exp.	Calc.[a]	Exp. $H_2C_3H^+$-N_2[d]	Exp. $H_2C_3H^+$-Ne[d]
$\nu_1(a_1)$	C−H stretch	3320	3238[b]	3338		
$\nu_2(a_1)$	CH_2 sym. stretch	3072	3004[b]	3102	2897*	2912*
$\nu_3(a_1)$	C≡C stretch	2116	2077[b]	1893		
$\nu_4(a_1)$	CH_2 scissors	1500	1445[b]	1416		1346
$\nu_5(a_1)$	C−C stretch	1125	1122[b]	685	628	629
$\nu_6(b_1)$	CH_2 out-of-plane wag	1142	1111[b]	722		
$\nu_7(b_1)$	CCH out-of-plane bend	873	858[c]	514		
$\nu_8(b_1)$	CCC out-of-plane bend	268		263		
$\nu_9(b_2)$	CH_2 antisym. stretch	3171	3093[b]	3250		
$\nu_{10}(b_2)$	CH_2 in-plane wag	1059		998		
$\nu_{11}(b_2)$	CCH in-plane bend	627		680		
$\nu_{12}(b_2)$	CCC in-plane bend	283		245		

*tentative assignment

[a] RASSCF/cc-pVTZ calculations (unscaled)

[b] from IRPD spectrum of $H_2C_3H^+$-Ar (ref. 15)

[c] from photoelectron data (ref. 13)

[d] this work

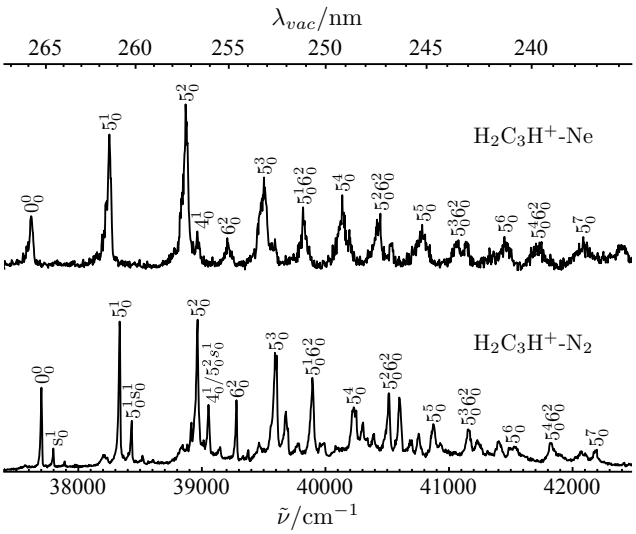


FIG. 2. The $\tilde{A}^1A_1 \leftarrow \tilde{X}^1A_1$ band system of $H_2C_3H^+$-Ne (top) and $H_2C_3H^+$-N_2 (bottom), recorded by monitoring $H_2C_3H^+$ photofragments as a function of laser wavelength.

B. Electronic spectra of $H_2C_3H^+$-Ne and $H_2C_3H^+$-N_2

The $\tilde{A}^1A_1 \leftarrow \tilde{X}^1A_1$ electronic spectra of $H_2C_3H^+$-Ne and $H_2C_3H^+$-N_2 over the 230–270 nm range are shown in Fig. 2. Measured peak positions are compiled in Table III, while fully assigned spectra are included in the SI. As observed by Wyss *et al.* for $H_2C_3H^+$ in a Ne matrix,[16] the $\tilde{A}^1A_1 \leftarrow \tilde{X}^1A_1$ band system is dominated by an extended progression with a spacing of $\approx$630 cm^{-1}. The $H_2C_3H^+$-N_2 and $H_2C_3H^+$-Ne spectra are very similar, although peaks in the $H_2C_3H^+$-N_2 spectrum are sharper and shifted to higher energy than their $H_2C_3H^+$-Ne counterparts. As well, the $H_2C_3H^+$-N_2 spectrum includes additional bands due to excitation of intermolecular modes, presumably the intermolecular stretch mode (ν_s). These transitions are discussed in Section IV E below. The origin transition for $H_2C_3H^+$-Ne occurs at $37\,618 \pm 15$ cm^{-1}, whereas the origin band for $H_2C_3H^+$-N_2 lies at $37\,703 \pm 15$ cm^{-1}, 85 cm^{-1} to higher energy. It is worth noting that the band origin for $H_2C_3H^+$ in a Ne matrix is shifted by 288 cm^{-1} to lower energy with respect to the origin of the $H_2C_3H^+$-Ne complex.

C. Main band assignments

The $H_2C_3H^+$-Ne and $H_2C_3H^+$-N_2 spectra are dominated by a single progression extending for at least 6 quanta. Previously, Wyss *et al.* argued that the main progression was due to

the ν_{11} CCH in-plane bending mode, that becomes Franck-Condon active in a distorted C_s excited $\tilde{A}^1A_1$ state.[16] Our RASSCF/cc-pVTZ calculations indicate that $H_2C_3H^+$ retains C_{2v} symmetry in the $\tilde{A}^1A_1$ state and that the progression arises from ν_5, primarily a C-C stretch vibration that drops in frequency from 1125 to 685 cm^{-1} upon electronic excitation with a concomitant increase in the C-C bond length (accounting for the extended 5_0^n progression).

Simulation of the spectrum using the RASSCF/cc-pVTZ geometrical parameters (Fig.1) and vibrational frequencies (Table II) supports assignment of the dominant progression to ν_5, although the length of the progression is overestimated with a better match to experiment being given for a 0.16 Å elongation of the C-C bond rather than the CCSDT/EOM-CCSDT value of 0.19 Å. Simulated spectra for a range of bond length changes are provided in the supplemental material.[29] Note that the assignment of the dominant progression to the ν_5 CC stretch vibrational mode is consistent with Wyss *et al.*'s observation of only a small reduction in the progression spacing following deuteration (667 cm^{-1} for $H_2C_3H^+$and 641 $cm^{-1}$for $D_2C_3D^+$).[16]

Aside from the dominant ν_5 progression, several weaker transitions also appear in the $H_2C_3H^+$-Ne and $H_2C_3H^+$-N_2 spectra. For $H_2C_3H^+$-Ne, a transition appears at 0_0^0+1346 cm^{-1} that can be assigned to the 4_0^1 transition (CH_2 symmetric bend mode), which has a calculated excited state frequency of 1416 cm^{-1}. Higher $4_0^15_0^n$ transitions eventually merge with the 5_0^{n+2} bands. The corresponding $4_0^15_0^n$ transitions of $H_2C_3H^+$-N_2 overlap with transitions involving the intermolecular stretch mode ($5_0^{n+2}s_0^1$) and are difficult to resolve.

Another prominent transition occurs at 0_0^0+1585 cm^{-1} for $H_2C_3H^+$-Ne and 0_0^0+1576 cm^{-1} for $H_2C_3H^+$-N_2, approximately midway between the 5_0^2 and 5_0^3 transitions. Assignment of this band is uncertain. The only possible mode of a_1 symmetry is ν_3 (C≡C acetylenic stretch), which has a calculated excited state frequency of 1893 cm^{-1}, 315 cm^{-1} or 20% higher than the observed spacing, making it unlikely that it is responsible for the band. Alternatively, the 0_0^0+1585 cm^{-1} transition may correspond to two quanta of a vibrational mode with b_1 or b_2 symmetry and with a frequency of ≈790 cm^{-1}. On the basis of the calculated frequencies, the most likely mode is the ν_6 (b_1) CH_2 out-of-plane wag. As well, the substantial reduction in ν_6 frequency between the $\tilde{X}$ and $\tilde{A}$ states (from 1142 to 722 cm^{-1}), means that the 6_0^2 transition has appreciable intensity. This assignment implies that the RASSCF/cc-pVTZ ν_6 frequency underestimates the actual value by around 10%, suggesting that ν_6 possesses substantial negative anharmonicity, or that this mode is substantially affected by dynamical

correlation effects not captured by methods like RASSCF or CASSCF.

Evidence for the activity of other a_1 vibrational modes (*eg.* the ν_1 acetylenic and ν_2 methylenic C-H stretches) is equivocal. A peak appearing at 0_0^0+2912 cm^{-1} for $H_2C_3H^+$-Ne and 0_0^0+2897 cm^{-1} for $H_2C_3H^+$-N_2 can tentatively be assigned to the 2_0^1 transition (CH_2 symmetric stretch), while a band assignable to the $2_0^1 5_0^1$ transition is also observed for both molecules. These assignments imply a ν_2 frequency $\approx$200 cm^{-1} lower than the calculated excited state value (3102 cm^{-1}).

D. $H_2C_3H^+$-Ne spectrum

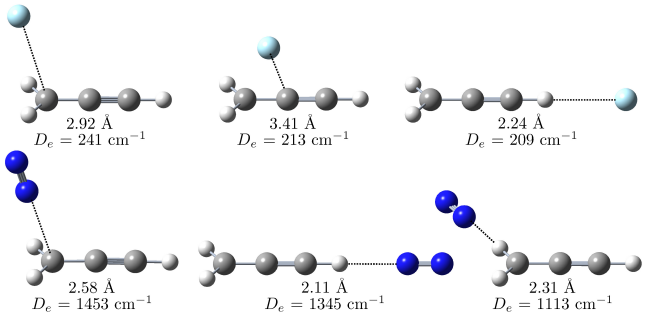


FIG. 3. Most stable structures for $H_2C_3H^+$-Ne (top) and $H_2C_3H^+$-N_2 (bottom). Dissociation energies (D_e) and intermolecular distances calculated at the CCSD(T*)-F12a level (from ref. 9) are indicated for each structure.

Having considered the main features of the $H_2C_3H^+$ electronic spectrum we turn now to a brief discussion of the properties of the $H_2C_3H^+$-Ne and $H_2C_3H^+$-N_2 species. The best guide to the structures and energetics of the two complexes comes from the CCSD(T*)-F12a level calculations by Botschwina *et al.*, who predicted three stable isomers for each species (see Fig. 3).[9] For the lowest energy $H_2C_3H^+$-Ne isomer, the C-bound isomer, the Ne atom resides above the molecular plane, adjacent the methylenic carbon (C_s symmetry, D_e=241 cm^{-1}). Lying slightly higher in energy is the in-plane isomer, with the Ne atom situated in the molecular plane closest to a methylenic hydrogen (C_s symmetry, D_e=213 cm^{-1}). Having a similar energy is an H-bound isomer with the Ne atom lying on the C_2 axis adjacent to the acetylenic hydrogen (C_{2v} symmetry, D_e=209 cm^{-1}). The 3 isomers of $H_2C_3H^+$-Ne are shown in Fig. 3.

It is not clear which $H_2C_3H^+$-Ne isomer is responsible for the observed electronic spectrum. Because only one series of peaks is seen, either there is only a single contributing isomer or the different isomers have similar electronic transition frequencies. Indeed it is conceivable that the asymmetric bands, which are shaded to lower energy, and have widths of $\approx$50 cm^{-1}, reflect the overlapping absorptions of isomers with slightly different band shifts.

E. $H_2C_3H^+$-N_2 spectrum

According to the calculations of Botschwina *et al.*,[9] $H_2C_3H^+$-N_2 has three stable isomers possessing similar structures to the $H_2C_3H^+$-Ne isomers, but with significantly higher dissociation energies (see Fig. 3). The lowest energy C-bound $H_2C_3H^+$-N_2 isomer (C_s symmetry, D_e=1453 cm^{-1}), H-bound isomer (C_{2v} symmetry, D_e=1345 cm^{-1}), and in-plane isomer (C_s symmetry, D_e=1113 cm^{-1}).[9] On the basis of measured infrared band intensities Dopfer *et al.* estimated a population ratio of 2:1 for C-bound versus H-bound forms of $H_2C_3H^+$-N_2, consistent with their relative binding energies and presence of two C-bound minima (N_2 above and below the plane) and only a single H-bound minimum on the $H_2C_3H^+$+N_2 PES.[9] Most of the features in the $H_2C_3H^+$-N_2 spectrum shown in Fig. 3 can be convincingly assigned to a single isomer. However, depending on the backing pressure and distance between the nozzle and electron impact zone, additional peaks appear, shifted to lower energy from the dominant peaks by $\approx$130 cm^{-1}. These peaks are presumably associated with a second isomer (see Fig. 4). At this stage we are unsure which of the three isomers is responsible for each set of peaks. Clarification of the peak assignments may be possible through IR-UV hole-burning experiments. If the assignments of Dopfer *et al.* are correct, the H-bound and C-bound forms have ν_1 CH stretch absorptions at 3139 and 3243 cm^{-1}, respectively.[9] Excitation of one of these IR bands should deplete the dominant UV transitions.

As mentioned above, the $H_2C_3H^+$-N_2 spectrum contains weak transitions spaced by +95 and +187 cm^{-1} with respect to the main transitions (see Fig. 4) that are absent from the $H_2C_3H^+$-Ne spectrum, and are most likely due to excitation of intermolecular modes, particularly the intermolecular stretch vibrational mode (ν_s), which according to DFT calculations (ωB97XD/aug-cc-pVTZ) has a frequency of 103 cm^{-1} for the linear H-bonded isomer, 93 cm^{-1} for the C-bound isomer, and 91 cm^{-1} for the in-plane isomer (see SI). It is also conceivable that the bands are associated with an a' intermolecular bending mode for the

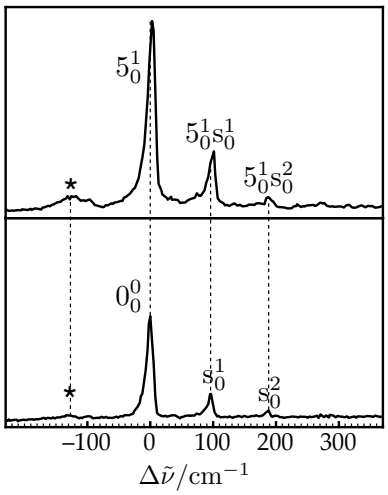


FIG. 4. Expanded view of the 0_0^0 and 5_0^1 peaks of $H_2C_3H^+$-N_2 showing transitions involving the intermolecular stretch mode (s_0^1 and s_0^2). Transitions assigned to a second isomer are denoted with an asterisk.

C-bound $H_2C_3H^+$-N_2 isomer. For example, the a' intermolecular bending modes of the C-bound isomer have predicted frequencies of 51 and 133 cm^{-1}, respectively. fgr:spectra

It is obvious that the vibronic bands of $H_2C_3H^+$-Ne are broader than those of $H_2C_3H^+$-N_2 (see Fig. 2). As mentioned in the preceding section, the broad asymmetric bands of $H_2C_3H^+$-Ne may reflect overlapping absorptions of several different isomers. It is also possible that the $H_2C_3H^+$-Ne complexes are warm and have quanta in the intermolecular stretch and bend vibrational modes, and that the observed bands are composed of overlapping hot bands of the type (s_1^1, s_2^2, b_1^1, b_2^2 etc.) that are progressively displaced to lower frequency due to a shallower excited state intermolecular potential energy surface. In the case of $H_2C_3H^+$-N_2, one might expect that the intermolecular modes will have higher frequencies, so that the hot bands will be less prominent.

V. SUMMARY AND CONCLUSIONS

Electronic spectra of the mass-selected $H_2C_3H^+$-Ne and $H_2C_3H^+$-N_2 complexes have been measured over the 230–270 nm range by monitoring their photodissociation in a tandem mass spectrometer. A prominent band system is observed corresponding to the $\tilde{A}^1A_1 \leftarrow \tilde{X}^1A_1$ transition, with an origin at $37\,618 \pm 15\,\mathrm{cm}^{-1}$ for $H_2C_3H^+$-Ne and $37\,703 \pm 15\,\mathrm{cm}^{-1}$ for $H_2C_3H^+$-N_2. In both cases, the $\tilde{A}^1A_1 \leftarrow \tilde{X}^1A_1$ band system exhibits well resolved vibronic structure,

which is deciphered with the use of electronic structure calculations. The strong Franck-Condon active mode, previously assigned to a CCH in-plane bend mode,[16] has been re-assigned to the ν_5 C–C stretch mode, consistent with the propargyl cation retaining C_{2v} symmetry in the excited state.

Hopefully, the current work will encourage measurement of the electronic spectrum for bare $H_2C_3H^+$ in the gas phase. A single Ne atom should be a benign tag having little effect on the electronic absorptions of the propargyl cation and it would be surprising if the transitions of the bare $H_2C_3H^+$ molecule were displaced by more than $50\,cm^{-1}$ from those of $H_2C_3H^+$-Ne. The current work also establishes foundations for IR-UV hole-burning experiments to help disentangle the rather complicated $C_3H_3^+$-N_2 IR spectrum which has been postulated to include bands from several isomers in which N_2 is attached to $H_2C_3H^+$and c-$C_3H_3^+$ at different sites.

ACKNOWLEDGMENTS

This research was supported under the Australian Research Council's Discovery Project funding scheme (Project Numbers DP110100312 and DP120100100). The computations were undertaken using resources provided by the NCI National Facility through the National Computational Merit Allocation Scheme supported by the Australian Government, and resources provided by the Victorian Life Sciences Computation Initiative. We would like to thank J. F. Stanton (University of Texas, Austin) for helpful discussions on the convergence of EOM methods with excitation level and for providing access to features not yet in the released version of CFOUR.

REFERENCES

[1]F. P. Lossing, Can. J. Chem. **50**, 3973 (1972).

[2]M. J. McEwan, C. L. McConnell, C. G. Freeman, and V. G. Anicich, J. Phys. Chem. **98**, 5068 (1994).

[3]J. M. Goodings, D. K. Bohme, and N. Chun-Wai, Combust. Flame **36**, 27 (1979).

[4]J. H. Waite Jr., You, T. E. Cravens, A. J. Coates, F. J. Crary, B. Magee, and J. Westlake, Science **316**, 870 (2007).

[5]A. Korth, M. L. Marconi, D. A. Mendis, F. R. Krueger, A. K. Richter, R. P. Lin, D. L. Mitchell, K. A. Anderson, C. W. Carlson, H. Reme, J. A. Sauvaud, and C. d'Uston, Nature **337**, 53 (1989).

[6]E. Herbst, N. G. Adams, and D. Smith, Astrophys. J. **269**, 329 (1983).

[7]P. Thaddeus, J. M. Vrtilek, and C. A. Gottlieb, Astrophys. J. **299**, L63 (1985).

[8]P. Botschwina, R. Oswald, and G. Rauhut, Phys. Chem. Chem. Phys. **13**, 7921 (2011).

[9]P. Botschwina, R. Oswald, and O. Dopfer, Phys. Chem. Chem. Phys. **13**, 14163 (2011).

[10]X. Huang, P. R. Taylor, and T. J. Lee, J. Phys. Chem. A **115**, 5005 (2011).

[11]Z. Pachuau, K. S. Kharnaior, and R. H. D. Lyngdoh, J. Chem. Sci. **125**, 365 (2013).

[12]D. W. Minsek and P. Chen, J. Phys. Chem. **94**, 8399 (1990).

[13]H. Gao, Z. Lu, L. Yang, Z. J., and C. Y. Ng, J. Chem. Phys. **137**, 161101 (2012).

[14]O. Dopfer, D. Roth, and J. P. Maier, Int. J. Mass Spectrom. **218**, 281 (2002).

[15]A. M. Ricks, G. E. Douberly, P. v. R. Schleyer, and M. A. Duncan, J. Chem. Phys. **132**, 0511011 (2010).

[16]M. Wyss, E. Riaplov, and J. P. Maier, J. Chem. Phys. **114**, 10355 (2001).

[17]M. A. Duncan, J. Phys. Chem. A **116**, 11477 (2012).

[18]D. A. Wild and E. J. Bieske, Int. Rev. Phys. Chem. **22**, 129 (2003).

[19]V. Dryza, N. Chalyavi, J. Sanelli, and E. Bieske, J. Chem. Phys. **137**, 204304 (2012).

[20]V. Dryza, J. A. Sanelli, E. G. Robertson, and E. J. Bieske, J. Phys. Chem. A **116**, 4323 (2012).

[21]N. Chalyavi, V. Dryza, J. A. Sanelli, and E. J. Bieske, J. Chem. Phys. **138**, 224307 (2013).

[22]J. Olsen, B. O. Roos, P. Jørgensen, and H. J. A. Jensen, J. Chem. Phys. **89**, 2185 (1988).

[23]K. Aidas, C. Angeli, K. L. Bak, V. Bakken, R. Bast, L. Boman, O. Christiansen, R. Cimiraglia, S. Coriani, P. Dahle, E. K. Dalskov, U. Ekström, T. Enevoldsen, J. J. Eriksen, P. Ettenhuber, B. Fernández, L. Ferrighi, H. Fliegl, L. Frediani, K. Hald, A. Halkier, C. Hättig, H. Heiberg, T. Helgaker, A. C. Hennum, H. Hettema, E. Hjertenæs, S. Høst, I.-M. Høyvik, M. F. Iozzi, B. Jansík, H. J. Aa. Jensen, D. Jonsson, P. Jørgensen, J. Kauczor, S. Kirpekar, T. Kjærgaard, W. Klopper, S. Knecht, R. Kobayashi, H. Koch, J. Kongsted, A. Krapp, K. Kristensen, A. Ligabue, O. B. Lutnæs, J. I. Melo, K. V. Mikkelsen, R. H. Myhre, C. Neiss, C. B. Nielsen, P. Norman, J. Olsen, J. M. H. Olsen, A. Osted, M. J. Packer, F. Pawlowski, T. B. Pedersen, P. F. Provasi, S. Reine, Z. Rinkevicius, T. A. Ruden, K. Ruud, V. V. Rybkin, P. Sałek, C. C. M. Samson, A. S. de Merás, T. Saue, S. P. A.

Sauer, B. Schimmelpfennig, K. Sneskov, A. H. Steindal, K. O. Sylvester-Hvid, P. R. Taylor, A. M. Teale, E. I. Tellgren, D. P. Tew, A. J. Thorvaldsen, L. Thøgersen, O. Vahtras, M. A. Watson, D. J. D. Wilson, M. Ziolkowski, and H. Ågren, WIREs Comput. Mol. Sci. **4**, 269 (2014).

[24]CFOUR, a quantum chemical program package written by J.F. Stanton, J. Gauss, M.E. Harding, P.G. Szalay with contributions from A.A. Auer, R.J. Bartlett, U. Benedikt, C. Berger, D.E. Bernholdt, Y.J. Bomble, L. Cheng, O. Christiansen, M. Heckert, O. Heun, C. Huber, T.-C. Jagau, D. Jonsson, J. Jusélius, K. Klein, W.J. Lauderdale, D.A. Matthews, T. Metzroth, L.A. Mück, D.P. O'Neill, D.R. Price, E. Prochnow, C. Puzzarini, K. Ruud, F. Schiffmann, W. Schwalbach, C. Simmons, S. Stopkowicz, A. Tajti, J. Vázquez, F. Wang, J.D. Watts and the integral packages MOLECULE (J. Almlöf and P.R. Taylor), PROPS (P.R. Taylor), ABACUS (T. Helgaker, H.J. Aa. Jensen, P. Jørgensen, and J. Olsen), and ECP routines by A. V. Mitin and C. van Wüllen. For the current version, see http://www.cfour.de.

[25]R. S. Mulliken, J. Chem. Phys. **23**, 1997 (1955).

[26]J. D. Chai and M. Head-Gordon, Phys. Chem. Chem. Phys. **10**, 6615 (2008).

[27]N. Chalyavi, K. J. Catani, J. A. Sanelli, V. Dryza, and E. J. Bieske, Mol. Phys. **113**, 2086 (2015).

[28]M. J. Frisch, G. W. Trucks, H. B. Schlegel, G. E. Scuseria, M. A. Robb, J. R. Cheeseman, G. Scalmani, V. Barone, B. Mennucci, G. A. Petersson, H. Nakatsuji, M. Caricato, X. Li, H. P. Hratchian, A. F. Izmaylov, J. Bloino, G. Zheng, J. L. Sonnenberg, M. Hada, M. Ehara, K. Toyota, R. Fukuda, J. Hasegawa, M. Ishida, T. Nakajima, Y. Honda, O. Kitao, H. Nakai, T. Vreven, J. A. Montgomery, Jr., J. E. Peralta, F. Ogliaro, M. Bearpark, J. J. Heyd, E. Brothers, K. N. Kudin, V. N. Staroverov, R. Kobayashi, J. Normand, K. Raghavachari, A. Rendell, J. C. Burant, S. S. Iyengar, J. Tomasi, M. Cossi, N. Rega, J. M. Millam, M. Klene, J. E. Knox, J. B. Cross, V. Bakken, C. Adamo, J. Jaramillo, R. Gomperts, R. E. Stratmann, O. Yazyev, A. J. Austin, R. Cammi, C. Pomelli, J. W. Ochterski, R. L. Martin, K. Morokuma, V. G. Zakrzewski, G. A. Voth, P. Salvador, J. J. Dannenberg, S. Dapprich, A. D. Daniels, Ö. Farkas, J. B. Foresman, J. V. Ortiz, J. Cioslowski, and D. J. Fox, "Gaussian 09 Revision A.1," Gaussian Inc. Wallingford CT 2009.

[29]See supplemental material at [URL will be inserted by AIP] for a compilation of calculated

vibrational frequencies for $H_2C_3H^+$, $H_2C_3H^+$-Ne and $H_2C_3H^+$-N_2, fully assiged spectra of $H_2C_3H^+$-Ne and $H_2C_3H^+$-N_2, and simulated spectra of $H_2C_3H^+$.

TABLE III. Measured transition frequencies and assignments for the $\tilde{A}^1A_1 \leftarrow \tilde{X}^1A_1$ band system of $H_2C_3H^+$-N_2 and $H_2C_3H^+$-Ne.

	$H_2C_3H^+$-N_2		$H_2C_3H^+$-Ne	
Assignment	$\tilde{\nu}$	$\Delta\tilde{\nu}$	$\tilde{\nu}$	$\Delta\tilde{\nu}$
0_0^0 iso 2	37569	-134	-	-
0_0^0	37703	0	37618	0
s_0^1	37797	95	-	-
s_0^2	37890	187	-	-
5_0^1 iso 2	38204	501	-	-
5_0^1	38334	631	38251	633
$5_0^1 s_0^1$	38432	729	-	-
$5_0^1 s_0^2$	38521	818	-	-
5_0^2 iso 2	38844	1141	-	-
5_0^2	38965	1262	38875	1257
4_0^1	-	-	38965	1346
$5_0^2 s_0^1$	39056	1353	-	-
$5_0^2 s_0^2$	39148	1445	-	-
6_0^2	39279	1576	39204	1585
5_0^3 iso 2	39467	1764	-	-
5_0^3	39596	1893	39500	1881
$4_0^1 5_0^1$	-	-	39583	1965
$5_0^3 s_0^1$	39680	1977	-	-
$5_0^3 s_0^2$	39781	2078	-	-
$5_0^1 6_0^2$	39895	2192	39824	2206
5_0^4 iso 2	40089	2386	-	-
5_0^4	40230	2527	40133	2514
$4_0^1 5_0^2$	-	-	40195	2577
$5_0^4 s_0^1$	40302	2599	-	-
$5_0^4 s_0^2$	40388	2685	-	-
$5_0^2 6_0^2$	40514	2811	40433	2815
2_0^{1*}	40600	2897	40530	2912
$5_0^5/6_0^4$	40876	3173	40777	3158
$5_0^3 6_0^2$	41159	3456	41071	3452
$2_0^1 5_0^{1*}$	41231	3528	41127	3508
5_0^6	41529	3826	41470	3851
$5_0^4 6_0^2/2_0^1 5_0^{2*}$	41823	4120	41734	4115
5_0^7	42189	4486	42085	4467

* tentative assignment